

SEPERATOR DESIGN CRITERIA FOR A SOLAR-HYDROGEN ELECTROCHEMICAL GENERATOR

S. Haussener^{1,2}, C. Xiang³, J. Spurgeon³, S. Ardon³, A. Weber¹, N. Lewis³

¹Lawrence Berkeley National Laboratory, Berkeley, CA 94720, USA

²École Polytechnique Fédéral de Lausanne, Department of Mechanical Engineering, 1015 Lausanne, Switzerland

³Beckman Institute and Kavli Nanoscience Institute, California Institute of Technology, Pasadena, CA 91125, USA

Introduction

Solar irradiation is the most abundant energy source available but it is distributed and intermittent, thereby necessitating its storage via conversion to a fuel (e.g., hydrogen). One possible route for direct solar-hydrogen production is through an integrated electrochemical device that uses light-capturing semiconductors in contact with electrodes to generate oxygen and hydrogen [1,2]. Key in such a device is balancing product crossover with Ohmic losses in the solution which necessitate higher photovoltages. Often these requirements are accomplished using a polymer-electrolyte separator [3], yet the exact material-property design targets are not definitively known. In this presentation, a validated multi-physics numerical model of an electrochemical solar-hydrogen generator is used to study its performance. Advantages and limitations concerning current efficiency, required photovoltage, and safety are investigated as a function of separator transport parameters which leads to general design guidelines. Systems including both porous and nonporous photoactive components are examined.

Reactor designs

Three different reactor designs are investigated in the study at hand. Design (i) consists of a multijunction photoactive electrode covered with catalyst on each side [4], (ii) consisting of photoanode and photocathode separated by a membrane [5], and (iii) consisting of photoelectrodes composed of micro wire arrays embedded in a proton conducting membrane [6]. Each of this electrode-separator/membrane-assembly (ES/MA) is immersed in a conducting water solution. Two-dimensional slices through the design are depicted in figure 1.

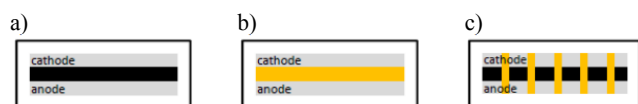
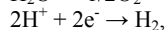
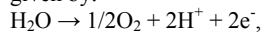


Figure 1. 2D slice through the container of conducting water solution and the ES/MA for designs (i)-(iii) in a)-c). Gray depicts electrodes, orange proton conducting membranes and black a non-conducting support.

Multi-physics model

A multi-physics model is developed solving for current and species conservation in the electrolyte and the (porous) electrodes and the (porous) membrane. The 3D model domain is depicted in figure 2. The electrochemical reactions at the anode and cathode are given by:



and are modeled by assuming Butler-Volmer kinetics (exchange current densities at anode and cathode are $1 \cdot 10^{-7} \text{A/cm}^2$ and $1 \cdot 10^{-3} \text{A/cm}^2$, respectively [7]), dependent on concentration for the anode side. The assumed boundary conditions are constant current densities

at the bottom of the electrode accounting for the produced current of the solar devices, and saturation and zero concentration of the produced species (hydrogen and oxygen) at the cathode and anode, respectively. Therefore any bubble formation and any effect of it on performance are neglected.

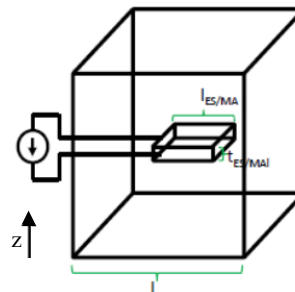


Figure 2. Computational domain for the multi-physics model consisting of a cubic container (edge length l) with immersed ES/MA (edge length $l_{\text{ES/MA}}$ and thickness $t_{\text{ES/MA}}$).

A measure of system's performance is the current efficiency, η_i , defined as

$$\eta_i = \frac{1}{V} \int_V \frac{i_v - i_{\text{co}}}{i_v} dV$$

where i_{co} is the crossover current given by $i_{\text{co}} = \nu F \dot{n}$ (ν : mole number, F : Farady constant, \dot{n} : molar flux). The Ohmic voltage drop, $\Delta\Phi_R$, in the solution given by the difference of the averaged potential of the liquid or electrolyte, Φ_l , at the two electrodes

$$\Delta\Phi_R = \frac{1}{V_a} \int_{V_a} \Phi_l dV - \frac{1}{V_c} \int_{V_c} \Phi_l dV$$

is used as an additional performance measure. The operational window for an efficient, cheap and working design is 0.99 current efficiency and 10mV Ohmic potential drop.

Results

Reference case. Design (i) is chosen as reference case due to its simplicity. The reference parameter for the model are: solution conductivity of 15S/m (corresponding to 0.5M H_2SO_4 solution), container edge length of 3cm, ES/MA edge length of 3mm and thickness of 100 μm (including two 20 μm electrodes) and electrode conductivity of 10^4S/m . Convection is neglected. Figure 3 depicts the electrolyte potential and the hydrogen concentration within the container. The reference case shows a current efficiency of 1 and an Ohmic potential drop of 31mV.

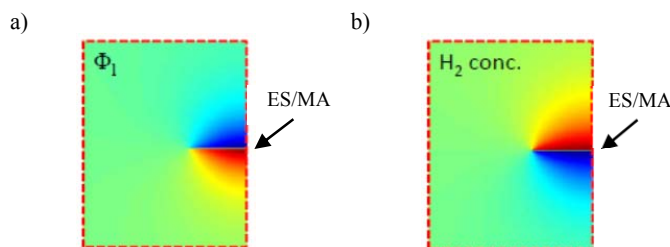


Figure 3. Electrolyte potential (a) and hydrogen concentration (b) in the container for design (i) with the reference parameters along a symmetry plane yz -plane.

Experimental comparison. The calculated Ohmic voltage drop over the electrode is compared to experimentally measured potential. For the experiment Pt is evaporated on each side of a glass slide and

the sides are electronically connected. Two reference luggin electrodes of Ag/AgCl in glass tubes filled with the same sulfuric acid electrolyte were prepared. The luggins are positioned at each side of the electrode and measure the potential difference at discrete points for different applied current densities. The potential drop calculated and measured are depicted in figure 4.

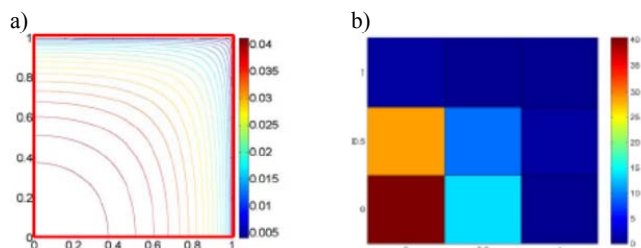


Figure 4. Spatial distribution of Ohmic potential calculated (inV) (a) and experimentally measured (in mV) (b) over one quarter of the electrode.

Geometrical optimization. The results for the geometrical optimization of the design by means of varying ES/MA length and thickness are depicted in figure 5. Decreasing ES/MA length leads to the decreasing Ohmic potential drop while the current efficiency decreases. The same trend is observed when decreasing thickness of the ES/MA. Design (i) does not allow for operation in the desired operational window.

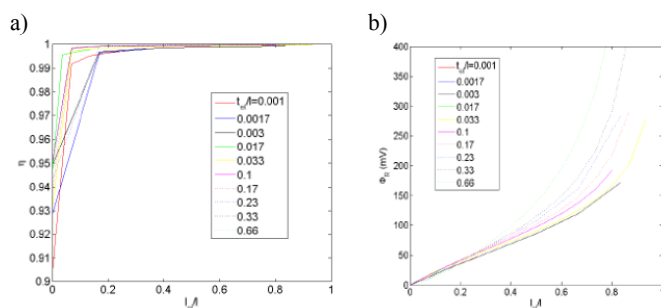


Figure 5. Current efficiency (a) and Ohmic potential drop (b) as function of the container normalized ES/MA length, $l_{ES/MA}/l$, for different container length normalized ES/MA thicknesses, $t_{ES/MA}/l$.

ES/MA design optimization. Performance of design (i) and four variations of design (iii) are depicted in figure 6. The black dot indicates the performance of design (i). Design (iii) without membrane in the pores is one variation (described as D2) of design (iii). Additionally, a non-homogeneous distribution of the pores is investigated. The non-homogeneous case depicted in figure 6 has an ES/MA, which outer edges are only porous (36% of the total surface). The incident current density is linearly decreased with 1-porosity as the surface area is reduced. A porous ES/MA leads to a reduced Ohmic potential drop of one order of magnitude but additionally also a significant decrease in current efficiency. This decrease can be limited when having an ES/MA only porous in its outer edges with the disadvantage of an reduction by only a factor of two in Ohmic voltage drop. Design (iii) with a porosity below 0.2 allows to operate the device in the desired operational performance window.

Influence of convection. The performance of the devices is substantially decreased when including a convective flow due to pressure gradient evolving due to the rapid hydrogen production

kinetics. Assumed 1mbar pressure gradient over the device leads to a current efficiency of 0.97 for the reference case (neglecting convection shows current efficiency of 1) while a highly porous electrode leads to a current efficiency of 0.87.

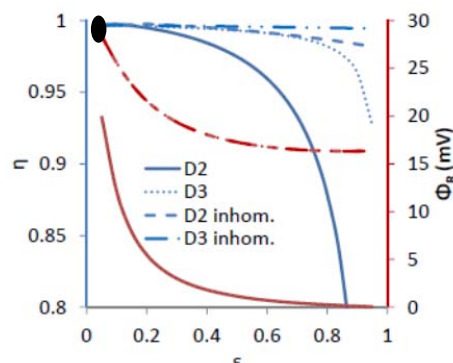


Figure 6. Current efficiency (left axis) and Ohmic voltage drop (right axis) as a function of the ES/MA porosity for design (iii) having no membrane in the pores (D2) or pores only in the outer edge of the ES/MA (inhom.).

Conclusions

A multi-physics model is developed for studying performance of different photoelectrochemical cells used to split water and produce hydrogen. The calculated performance of a reference design composed of a multijunction photoactive electrode covered with catalyst on each side immersed in conducting water solution is compared with experimental measurements of the Ohmic potential drop in the device and show acceptable agreement. Geometrical variation of the reference device shows that small electrode-separator-assemblies (ESA) are advantageous in regard of the Ohmic potential drop but also lead to significant reduction in current efficiency. Therefore design options with porous ESA, optionally immersed in proton conducting membrane, are proposed and compared showing reduced Ohmic potential drops but acceptable efficiency losses for porosities up to 20% compared to the reference case. The influence of convection due to pressure gradients in the device suggest significant reduction in the efficiency already for small pressure gradient (1mbar pressure gradient leads to current efficiencies of 0.97 compared to 1 for neglected convection).

Acknowledgement. This material is based upon work performed by the Joint Center for Artificial Photosynthesis, a DOE Energy Innovation Hub, supported through the Office of Science of the U.S. Department of Energy under Award Number DE-SC0004993.

References

- (1) Minggu, L. J.; Daud, W. R.; Kassim, M. B. *Int. J. of Hydrogen Energy*. **2010**, *35*, pp. 5233-5244.
- (2) Bak, T.; Nowotny, J.; Rekas, M.; Sorrell, C. C. *Int. J. of Hydrogen Energy*. **2002**, *27*, pp. 991-1022.
- (3) Carver, C.; Ulissi, Z.; Ong, C. K.; Dennison, S.; Kelsall, G. H.; Hellgardt, K. *Int. J. of Hydrogen Energy*. **2011**, pp. 1-13.
- (4) Nozik, A. J. *Appl Phys Lett*. **1977**, *30*, pp. 567-569.
- (5) Kainthla, R. C.; Khan, S. U. M.; Bockris, J. O. M. *Int. J. of Hydrogen Energy*. **2087**, *12*, pp. 381-392
- (6) Kelzenberg, M. D.; Turner-Evans, D. B.; Putnam, M. C.; Boettcher, S. W.; Briggs, R. M.; Baek, J. Y.; Lewis, N. S.; Atwater, H. A. *Energy & Environmental Science*, **2011**, *4*, pp. 866-871.
- (7) Choi, P.; Bessarabov, D. G.; Datta, R. *Solid State Ionics*, **2004**, *175*, pp. 535-539.